applied sciences

MDPI

Article

Virtual PLC Lab Enabled Physical Layer Improvement Proposals for PRIME and G3-PLC Standards

Asier Llano [1,*], Itziar Angulo [2], David de la Vega [2] and Laura Marron [1]

[1] Department of R&D, ZIV Automation, 48170 Zamudio, Spain; laura.marron@zivautomation.com
[2] Bilbao Faculty of Engineering, University of the Basque Country (UPV/EHU), 48013 Bilbao, Spain; itziar.angulo@ehu.eus (I.A.); david.delavega@ehu.eus (D.d.l.V.)
* Correspondence: asier.llano@zivautomation.com; Tel.: +34-663-057-794

Received: 24 January 2020; Accepted: 25 February 2020; Published: 4 March 2020

Abstract: Narrowband (NB) powerline communication (PLC) is extensively adopted by utilities for the communication in advanced metering infrastructure (AMI) systems. PLC technology needs to overcome channel disturbances present in certain grid segments. This study analyzes improvement proposals of the physical layer of the main narrowband PLC technologies approved by international communication organizations that are currently deployed in Europe: Powerline Intelligent Metering Evolution (PRIME) 1.3.6, PRIME 1.4, and G3-PLC, in order to improve PLC performance under channel disturbances. This thorough study is based on simulations carried out by an innovative ad hoc Virtual PLC Lab, developed by the authors, applied in replicable, fully-automated, and cost reduced test scenarios. The analysis is performed by applying standardized test methods and metrics, and by evaluating the influence of a set of representative channel disturbances defined by the European Telecommunications Standards Institute (ETSI) and selected noises generated by distributed energy resources (DER) in normal operation. PLC performance improvements in terms of equalizer curve fitting, error correction codes, and noisy subcarrier suppression mechanisms are presented. The performance gain due to each physical improvement proposal is accurately measured and compared under the same conditions in a replicable and automated test environment in order to evaluate the use of the proposals in the evolution of future PLC technologies.

Keywords: equalization; G3-PLC; modulation; OFDM physical layer; PLC for smart grids; powerline communication; PRIME 1.4; Reed–Solomon; spline; tone map

1. Introduction

Advanced metering infrastructure (AMI) deployments have changed the perception of the low voltage (LV) distribution grid. Smart meters scattered over the network offer LV grid visibility and accessibility. Distribution companies are now able to go one step beyond towards an advanced real-time representation, visibility, control, operation, and management of the LV network. LV narrowband (NB) powerline communication (PLC) is the most extended solution for the communication in these AMI systems [1]. Focusing on NB PLC technologies deployed in Europe, Powerline Intelligent Metering Evolution (PRIME) and G3-PLC are the most common standards [1].

The downside of this solution is that the electricity network is a complex communication channel with interferences and disturbances introduced by other devices connected to the network. In the LV grid, there is a very large variety of types and levels of disturbances in the communication channel, mainly classified by propagation channel effects, interfering noise, and non-intentional emissions. This variety, together with the high number of configurations of the communication technologies, complicates the detailed study of the effects of each types of disturbance on the different configurations.

As a result, sophisticated test methods are needed to evaluate, first, the effects of each type of disturbance on the different configurations of the communications technologies and, second, the efficiency of the strategies designed to overcome such disturbances.

This paper proposes the use of a Virtual PLC Lab to evaluate the performance of several improvement proposals for several PLC technologies. The Virtual PLC Lab includes the whole communication system, composed not only of transmission and reception devices, but also on the characterization of the different effects of the propagation channel. As a result, it enables an efficient analysis of new coding or equalizing techniques that would require long and complex validation procedures, without the need of physically implementing these techniques in the hardware devices, reducing the time and the cost of these developments.

Several articles study the NB PLC performance from 3 to 500 kHz in the presence of noise and harsh situations. This performance has been studied from multiple approaches. There are analytical studies based on generic PLC technologies [2]. Several studies are oriented to PRIME statistical performance in field setups [3,4]. Some specific studies focus on upper layer performance instead of being physical layer-oriented [5]. There are some comparisons of the performance of PLC technologies and physical layers, although these are not exactly under the same conditions [6]. Moreover, there is a lack of studies covering the PRIME standard in its recent 1.4 version and G3-PLC coherent modes [7]. Additionally, when disturbances are evaluated, no standard and controlled noise patterns are referenced [8]; moreover, the laboratory setups used in these studies are not reproducible, as no standard environments are utilized to determine PLC performance [9]. All these partial analyses demonstrate the need of developing simulation-based test benches for the design and validation of both the effects of channel disturbances and the performance of new techniques to improve the data transmission under these harsh conditions.

In view of the limitations of the available studies, the authors of the present contribution carried out a complete physical layer performance evaluation of the influence of real-world disturbances over PLC technologies within European Committee for Electrotechnical Standardization (CENELEC) A band (9–95 kHz) [10]. The work analyzed the impact of standard and controlled noise patterns over PRIME 1.3.6 [11], PRIME 1.4 [12], and G3-PLC [13,14] technologies under a reproducible and standard environment [15]. The study concluded with lessons to be learned for future technologies, opening several optimization lines [10]. This paper will, therefore, explore the main optimization lines identified in [10], suggesting improvement options for PRIME and G3-PLC standards and evaluating the performance enhancements obtained for the proposed modifications. This study is limited to the CENELEC A band, where most of the selected noise samples are more critical to the physical layer performance, and so that physical layer optimization proposals can be compared against the results in [10].

2. Objectives and Scope

Focused on the improvement lines identified in [10], this research work covers two main objectives. Firstly, the aim is to define improvement proposals for the physical layers of PRIME 1.3.6 [11], PRIME 1.4 [12], and G3-PLC [13,14] technologies, trying to improve their response against disturbances present in the LV grid. Secondly, the goal is to measure and evaluate the performance enhancement of each proposed physical layer modifications following standardized test method and metrics according to European Telecommunications Standards Institute (ETSI) Technical Specification (TS) 103 909 v1.1.1 [16] and using a set of representative channel disturbances.

The work will be organized as follows: Based on the PLC performance results obtained in [10], several physical layer improvement proposals for PRIME and G3-PLC are identified in Section 3. For each physical layer parameter under test, their original status, their room for improvement and the improvement proposal will be described. Once the improvements are defined, Section 4 introduces the methodology for the performance analysis of these physical layer modification proposals. Following this methodology, unitary results of each physical layer improvement are presented and discussed in

Section 5. Section 6 extracts the main highlights of the PLC physical layer improvements under test. This study concludes in Section 7 exploring possibilities for future studies.

3. Physical Layer Improvement Proposals for PRIME and G3-PLC

Based on the future evolutions concluded in [10], three improvement proposals are selected for the physical layer of PRIME 1.3.6 [11], PRIME 1.4 [12], and G3-PLC [13,14] technologies, trying to improve their response against the disturbances present in LV grids. Two types of improvement are studied: implementation changes within the scope of the standard, and proposals for the modification of PLC specifications.

1. PRIME implementation option: Improvement of the equalizer curve fitting.
2. PRIME modification to the standard: Reed–Solomon outer encoder as an addition to the convolutional encoder.
3. G3-PLC implementation option and modification to the standard: Implementation of tone mapping as defined in the standard, and proposal of technical improvements beyond the standard Tone Mapping.

3.1. PRIME: Equalizer

In a real propagation environment, the in-phase and quadrature (IQ) symbols extracted from the PLC signal appear distorted, due to the frequency response of the channel. This channel response may be estimated so the receiver is able to unmake that distortion and recover the transmitted data. That is the role of the equalizer, which will estimate the channel response using the pilot subcarriers in the header of the received frames. PRIME uses intercarrier differential modulations, which make it possible to decode its frames without channel estimation. Nevertheless, the equalization is intended to help in aligning the IQ symbols before soft decoding, reducing the error probability. However, using the pilot subcarriers for estimating the channel response has two drawbacks: the pilot subcarriers are not present in all the frequencies, and these samples are also distorted by the noise in the network.

The equalizer will therefore need to extrapolate and estimate the complete channel response, based on the pilot subcarriers, which are discrete and impaired by disturbances. The channel estimation performs curve fitting, in order to estimate the parts of the channel where there is no pilot subcarrier information, and in order to smooth the effect of the noise impact in the pilot subcarriers information. The equalizer performance, its ability to represent accurately the channel response and its immunity level against noise will depend on the curve model selected for the fitting.

For the previous PRIME study published in [10], a complex polynomial curve of degree 3 was selected to model the channel frequency response. The degree 3 was selected as a compromise between curve adaptability and stability. The coefficients are extracted through Least Square curve fitting, using the response of the pilot carriers as input. Polynomial curves, especially at higher degrees, might have negative properties. Figure 1 depicts the Runge effect, where small variations in the sampling of pilot subcarriers may cause large oscillations in the curves, increasing the resultant fluctuation with the degree of the polynomial.

An alternative spline curve model will be studied for the channel estimation of the equalizer. This first identified improvement is an implementation option of the receiver, and as such, it does not modify the transmitted signal and is transparent to the PRIME standard.

Studies available regarding interpolation based on spline curves are oriented to generic orthogonal frequency division multiplexing (OFDM) systems with diverse applications [16], but no studies particularizing the usage of spline curves on narrowband PLC systems have been found.

A spline is a function defined in segments formed by pieces of polynomials. Figure 2 shows a flat channel frequency response impaired by tonal noise, so that the 25th pilot subcarrier contains distorted information. The figure shows how spline estimation keeps a transfer function more stable for frequencies farther from the tonal noise. By contrast, with a polynomial curve, the noise affects a wider set of frequencies that are located farther from the tonal noise.

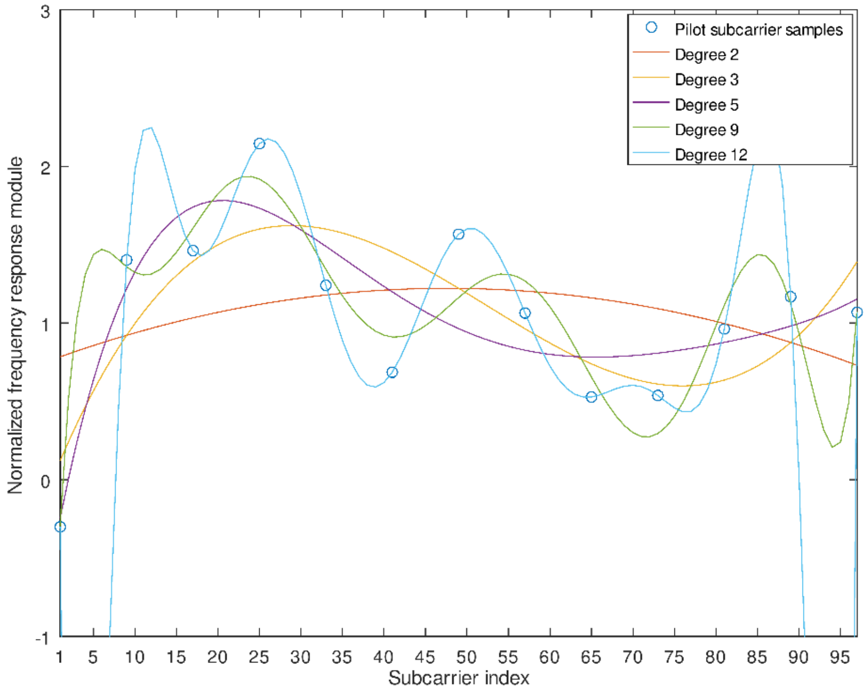

Figure 1. Obtained least square curve fitting for different degrees of the polynomial curve. The values in the Y-axis are given in linear units and normalized to the average frequency response.

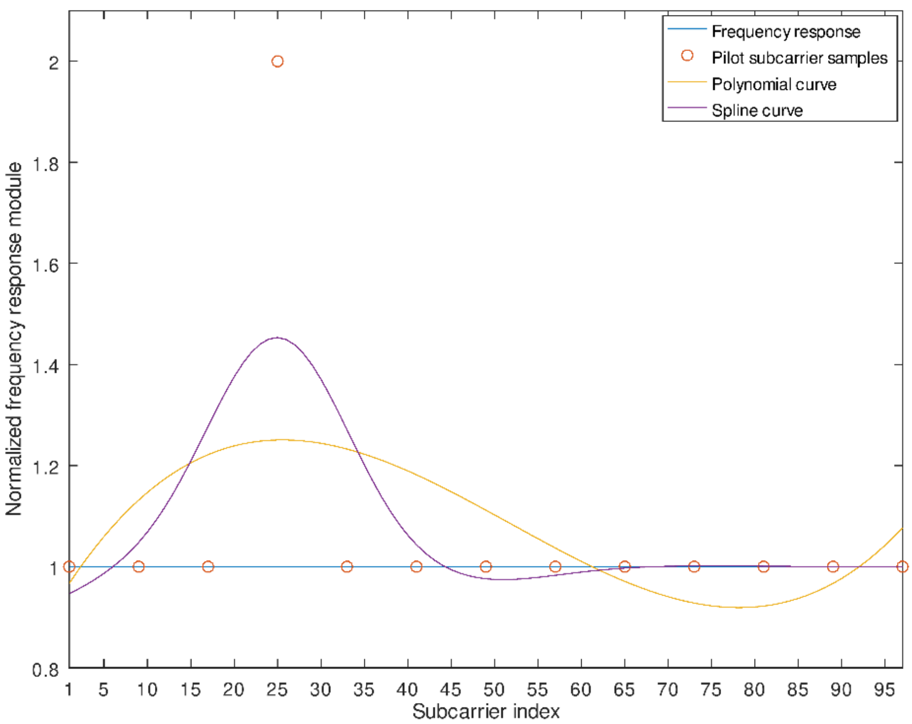

Figure 2. Comparison of spline (purple) and polynomial curve fitting (yellow) channel estimation, over a flat channel frequency response (blue) whose pilot tones (red) are impaired by tonal noise. The values in the Y-axis are given in linear units and normalized to the average frequency response.

3.2. PRIME: Reed–Solomon Encoding

PRIME specification defines an optional convolutional encoder for certain modulation schemes. A previous study from the authors concluded that modulation schemes without convolutional encoder are not efficient for real field scenarios [10], an observation that is consistent with other studies [17,18].

Based on the results of [10], the use of G3-PLC Reed–Solomon outer encoder as an addition to PRIME convolutional encoder was identified as an interesting option. The Reed–Solomon error correction mechanism, as described in G3-PLC specification [13,14], will be analyzed, as a particularization of its generic definition [19]. Its normal mode of eight correctable symbols is selected, which is obtained with the introduction of 16 parity bytes.

Most PRIME hardware platforms also support G3-PLC with a firmware change. This means that the Reed–Solomon algorithm is already available without hardware modification.

Published studies oriented to G3-PLC and PRIME performance improvements mention the advantages of Reed–Solomon in G3-PLC compared to PRIME standard [8]. Nevertheless, they do not explore the possibility of adding Reed–Solomon to PRIME technology.

For this proposal, PRIME based transmitter and receiver are modified so that a Reed–Solomon encoder and decoder are introduced, as shown in Figures 3 and 4. This modification is introduced over the best PRIME implementation of the ones previously assessed, this is, including the spline curve model for the channel estimation of the equalizer described in the previous section. The convolutional decoder being used in the modems of this study and [10] are based on soft input Viterbi algorithm with Euclidean metric.

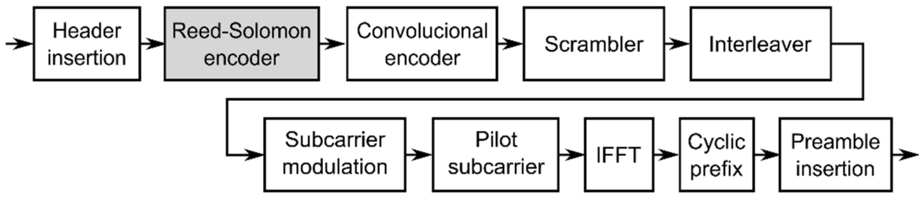

Figure 3. PRIME physical layer transmission diagram introducing Reed–Solomon.

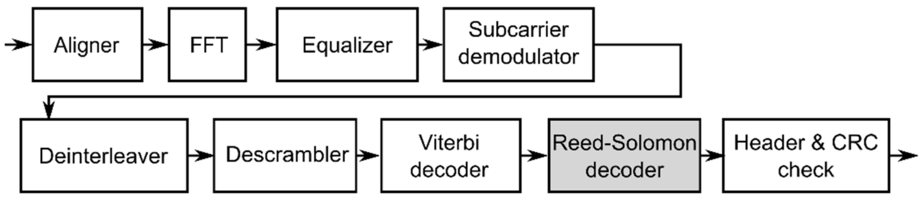

Figure 4. PRIME physical layer reception diagram introducing Reed–Solomon.

3.3. G3-PLC: Tone Map

G3-PLC technology includes in its specification [13,14] an adaptive mechanism named tone map. Based on channel estimation, the Tone Map identifies a list of subcarriers that can be affected by channel disturbances and, therefore, they will not be used to exchange data in the communication between two PLC modems.

The previous work published by the authors [10] did not implement the tone map option but highlighted the interest of analyzing its technical possibilities. This third improvement combines the study of this technique as defined in G3-PLC, with an evolution proposal that consists of redistributing the power of the unused subcarriers.

The study included in [20] evaluates the implementation limit of static subcarrier suppression or *notching* for G3-PLC manufacturers. However, the state of art of subcarriers suppression mechanisms does not analyze the unitary impact of the dynamic suppression tone map in G3-PLC technology.

3.3.1. Standard Tone Map

A tone map is defined as a six-bit field where each bit represents the content of a group of six subcarriers. If a bit is set to '1', its associated group of subcarriers are active for the payload and include data. If it is set to '0', they are inactive and a pseudo-random sequence is introduced instead

Whereas the standard definition limits tone map usage to non-robust modes, this study applies this technique to all modulation schemes.

Using a tone map means that fewer payload subcarriers are used for data exchange in the payload, requiring more OFDM symbols, resulting in lower system throughput for a certain modulation scheme.

The tone map used for this research work is obtained with the automatic tone map selection algorithm integrated in the G3-PLC modems. For this tone map autodetection algorithm security thresholds are defined for the average SNR of each modulation scheme, and represented in Table 1. For each modulation scheme, this minimum SNR is checked for each of the subcarrier groups. If the average SNR of the group is higher than the defined threshold, the bit that represents that group of subcarriers will be selected as '1', otherwise it will be '0'.

Table 1. SNR thresholds for tone map detection.

Modulation Scheme	SNR Threshold
Robo Coherent	2 dB
Robo Differential	3.5 dB
BPSK	5.5 dB
DBPSK	7.5 dB
QPSK	9 dB
DQPSK	11 dB
8PSK	14 dB
D8PSK	16 dB

This process for calculating the tone map is repeated for each available modulation scheme. The combination of the tone map and modulation scheme that has better throughput is selected. In a complete G3-PLC communication, this process would be invoked during the neighbor discovery process of the medium access control (MAC) layer.

The threshold values presented in Table 1 are between 4 and 6 dB higher than the minimum SNR required for the receiver to decode the frames in presence of AWGN noise [10]. This security margin is included in order to handle possible worse channel conditions not directly measurable by SNR, and to handle variations of the channel in time after its negotiation.

3.3.2. Reallocation of the Power Assigned to Inactive Tones

The specification of G3-PLC tone map defines that all the subcarriers transmit either data or a pseudo-random sequence. In this work, an alternative approach will be analyzed. P1901.2 [21] supports, for FCC and ARIB bands, the option of not introducing energy in inactive subcarriers. This nulling technique will be applied to G3-PLC CENELEC A band and will be extended reallocating that power within the rest of subcarriers. The total transmission power will be maintained constant, but the transmission power spectral density of the active carriers changes with the number of inactive subcarriers. The expected increase of the power spectral density for these subcarriers can be represented in dB as:

$$PSD_{TX} = 10 \cdot \log \frac{Number\ of\ inactive\ subcarriers}{Number\ of\ active\ subcarriers} \quad (1)$$

The impact of this power reallocation is depicted in Figure 5. It represents the spectral evolution of the payload for different tone map combinations, while the total power is kept constant to 120 dBμV.

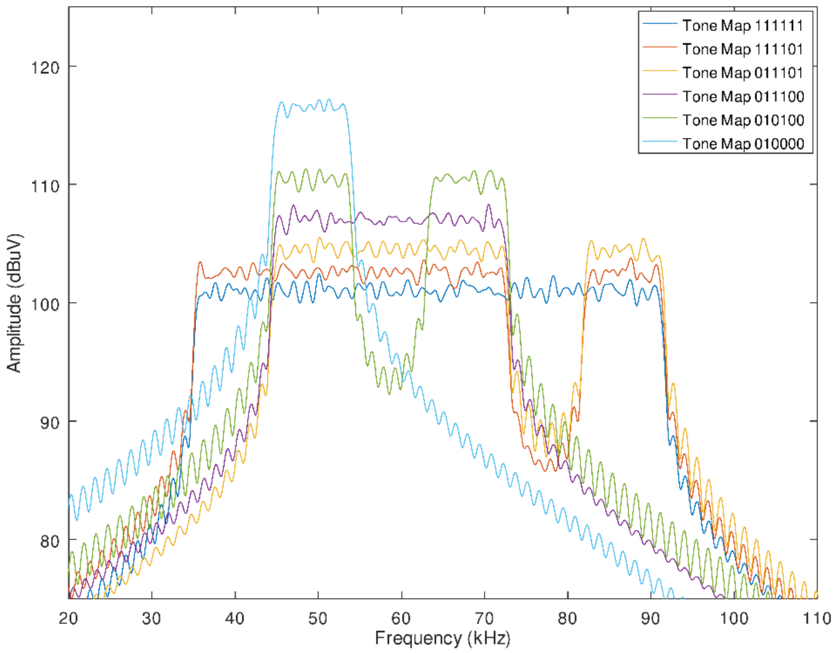

Figure 5. Payload spectral evolution using tone map power reallocation with 500 Hz frequency resolution and a total transmission power of 120 dBμV.

4. Methodology for the Performance Analysis of the Physical Layer Proposals

The methodology of this study is based on standardized procedure, test setup, and metrics. Moreover, the evaluated channel disturbances are divided into noises defined by ETSI and a selection of noises caused by distributed energy resources (DER) obtained from field trials. Additional details about the methodology can be found in a previous work from the authors [10].

4.1. Test Method and Setup Based on ETSI TS 103 909 v1.1.1 Integrated into a Virtual PLC Lab

ETSI TS 103 909 v1.1.1 [15] defines a standard and reproducible environment to determine the performance of narrowband PLC technologies under realistic channel conditions. It defines a test setup where a transmitter and receiver are connected independently, through a channel characterized by a nearly flat in-band frequency response, with controlled attenuation and additive noise sources and waveforms. This setup, described in detail in [15], is defined for a controlled alternating current (AC) mains environment, where the transmitter and receiver are connected through two isolated mains branches.

These standardized setup and environment are integrated into the Virtual PLC Lab [22], which is a fully automated, cost effective, and repeatable test environment. This is a system that replicates all the analogue elements of a PLC laboratory in digital technology. This tool runs multiple virtual PLC modems connected through a virtual digital medium with configurable characteristics, such as attenuation, noise patterns, and transfer function models. Each modem and the medium are software processes running in a computer. These processes interchange the digital representation of the PLC signals through UNIX sockets.

4.2. Standard and Controlled Channel Disturbances

The overall analysis comprises 38 disturbance input sources selected in [10] as a set of representative channel disturbances to be found in the LV distribution grid. First, the ETSI TS 103 909 v1.1.1 [15] standard defines a real-world noise collection composed of 31 waveforms, which are well defined, repeatable, and supported by the scientific community. This collection aims to represent the most challenging situations for PLC communications. Second, this set of noises is completed with a selection of disturbances generated by DER, which have demonstrated to be critical noise sources for PLC [23,24]. Therefore, the complete selection of disturbances is composed of:

- Twenty-five tonal noises (ETSI): Noise sources modeled come in the form of off-line AC switch-mode power converters.
- One periodic impulse noise (ETSI): Noise sources are generated by a triode for alternating current controlled lamp dimmer.
- One random impulse noise (ETSI): Series-wound AC motors are a very common source of this type of noise.
- Four intentional communicator noises (ETSI): Comprised of one waveform of a device complying with the ISO/IEC 14908-3 standard [25] and three waveforms of powerline intercoms (or baby monitors).
- Six DER noises (field measurements): The second source of representative noises was recorded in some field trials carried out close to several DER at facilities of the Centre for the Development of Renewable Energy Sources (CEDER) of the Research Centre for Energy, Environment and Technology (CIEMAT), a Spanish center for research, development and promotion of renewable energies [26]. A compilation of these noise recordings is available in [23,27]. The six noises are identified as *der04*, *der06*, *der34*, *der36*, *der50*, and *der51*.

Furthermore, the performance under additive white Gaussian noise is evaluated to serve as a reference whose results can be compared to other kinds of noise.

4.3. PLC Performance Metrics Based on ETSI TS 103 909 v1.1.1

The test metrics used for this PLC performance study are defined by ETSI TS 103 909 V1.1.1 [15]. The usage of these metrics is thoroughly described in [10]. These metrics are given in terms of the link budget and effective data rate.

Effective packet layer data rate (DR_{PKT}) [15] is the number of bits delivered to the data-link layer divided by a full formatted packet cycle time. It provides a measurement of the cost of the physical mechanisms in the data rate available to upper layers.

The link budget is a measure of how much signal attenuation can be present between transmitter and receiver such that a specified level of successful message delivery is achieved. That level of successful message delivery is established as a frame error rate (FER) of 5% [15]. As described in [10], given a physical configuration of the transmitter and a specific noise pattern, the Virtual PLC Lab calculates through iterations the minimum reception power that matches the target FER, which compared with the nominal transmission power provides the link budget.

ETSI TS 103 909 V1.1.1 [15] specifies link budget metrics for each of the disturbance types defined in the document and some composite ones:

- *Tonal noise link budget:* First, the 25 individual measured link budgets are calculated and identified as $LB_{tonal,i}$ for i from 1 to 25, corresponding to switching frequencies of $21 + 5 \cdot i$ kHz. These individually calculated link budgets are averaged. To provide added statistical weight to the most challenged result, while also considering the average, the overall tonal noise link budget is specified to be the lowest of the 25 individually measured link budgets, averaged with the previously calculated average, giving equal weight to those two figures.
- *Periodic impulse noise link budget:* Defined as the link budget measured in presence of the periodic impulse noise.
- *Random impulse noise link budget:* Defined as the link budget measured in presence of the random impulse noise.
- *Intentional communicator link budget:* Defined to be the smallest of the four individual intentional communicator link budget values.
- *Composite link budget* (LB_{PHY}): Defined to be the average of the following measurement values: *Unimpaired link budget* (obtained for a noiseless environment), *tonal noise link budget*, *periodic impulse*

noise link budget, *random impulse noise link budget*, and *intentional communicator link budget*. The *unimpaired link budget* averaged for the *composite link budget* is capped to 80 dB.

These metrics have been extended following the same approach to the non-intentional emissions selected from DER:

- *dernn link budget* (where *nn* is *04, 06 34 36, 50* and *51*): Each of these link budgets is defined as the link budget measured in presence of one of the der noises that gives its name.
- *der average link budget:* Defined to be the average of the six individual link budget values of DER.

The information given by these metrics is complemented with new metrics defined as part of the research process described in [10]:

- *Signal to Noise Ratio (SNR) required for AWGN:* The minimum SNR required in order to decode physical packets with FER lower than 5% in the presence of AWGN. Reference the metric for the analysis of the results.
- *Tonal in-band noise link budget:* A new metric defined in [10] to avoid the bias effect caused by some of the tonal noises included in [15] that are out of the bands of the communication systems under test. It considers only the disturbances in the communication band.
- *Composite in-band link budget:* In a similar way to the *tonal in-band noise link budget*, the aim is to avoid the bias effect of the high link budgets related to noises in frequencies outside the communication band.

4.4. Summary of Performed Simulations for G3-PLC and PRIME Technologies

PLC performance is measured with a complete implementation of physical layer modems in the Virtual PLC Lab, whose technology is certified by G3-PLC and PRIME Alliances. As such, the implementation includes realistic synchronization, frequency offset correction, and automatic gain control mechanisms. The comparison of the proposed improvements is carried out for all CENELEC-A modes available for G3-PLC and PRIME technologies and evaluated under the same circumstances. Tests are performed with 22 physical layer options configured in the Virtual PLC Lab:

- Eight options of the physical layer for G3-PLC: Four non-coherent and four coherent modes.
- Fourteen options of the physical layer for PRIME: Six modulation schemes for type A frames, which are common to PRIME 1.3.6 and 1.4 versions, and eight for type B, which is available only in PRIME 1.4 and introduces increased physical robustness.

Each of these configurations is evaluated under the 38 disturbances selected in [10], considered as a set of representative channel disturbances to be found in the LV distribution grid. For the above-mentioned configurations and for each channel disturbance, FER is evaluated per each SNR and the corresponding link budget is calculated.

For PRIME, the process is repeated twice: for the equalization improvement and Reed–Solomon improvement. Table 2 represents the different parameters used in [10] and the two additional simulation steps of this study.

Table 2. Simulation parameters and steps for PRIME.

	Equalization Curve	Forward Error Correction
Original [10]	Polynomial	Convolutional Coding
Equalizer improvement	Spline	Convolutional Coding
Reed–Solomon improvement	Spline	Convolutional Coding with Reed–Solomon

For G3-PLC, the process is executed three times: for tone map calculation, standard tone map testing and tone map with power reallocation evaluation. The tone map is calculated following the algorithm described in Section 3.3.1. The communication parameters are configured according to the communication limit defined by ETSI [15] (attenuation corresponding to FER 5% with tone map '111111'). The algorithm will then obtain the tone map value that improves the FER under these conditions. The different parameters used in [10] and the additional simulation steps of this study are summarized in Table 3.

Table 3. Simulation parameters and steps for G3-PLC.

	Tonemap Used	Power Reallocation
Original [10]	'111111'	No
Tonemap calculation	'111111'	No
Standard Tonemap	Calculated	No
Power reallocation	Calculated	Yes

In summary, this study involves 52 physical configuration options in channel conditions impaired by 38 disturbances. In total, the Virtual PLC Lab has generated 1782 FER-SNR curves whose calculations involved the exchange of 848 million frames.

5. Results and Discussion

This section summarizes the main results obtained for each of the improvement proposals under analysis. Additionally, these results are interpreted and discussed.

Two tables per improvement are presented, showing first the absolute obtained results and then offering the incremental results that quantify the performance improvement with respect to the initial configuration of the PLC technology under study. [15]. The rows of the tables include the test metrics listed in Section 4.3. This covers disturbance sources of ETSI and DER, metrics defined by ETSI, and additional metrics defined in [10].

The columns of the tables represent the modulation schemes of the physical layer defined for each PLC technology.

In most of the analysis, if not stated otherwise, the mean results are calculated by averaging the results of the *composite in-band link budget* and the *DER average link budget.*

5.1. PRIME: Equalizer

Table 4 collects the results with the alternative spline curve model for the channel estimation of the equalizer. Table 5 represents the incremental results compared to the initial configuration with a polynomial curve published in [10].

Table 4. Absolute results with the spline equalizer for PRIME 1.3.6 and 1.4.

	Header Type B *								Header Type A						
Parameter	Robust DBPSK	Robust DQPSK	DBPSK_CC	DQPSK_CC	D8PSK_CC	DBPSK	DQPSK	D8PSK	DBPSK_CC	DQPSK_CC	D8PSK_CC	DBPSK	DQPSK	D8PSK	Units
SNR required for AWGN	−1,0	1,8	3,2	6,0	11,0	9,2	14,6	20,2	3,6	6,4	11,0	9,2	14,6	20,0	dB
Packet layer data rate (DR_{PKT})	4,8	8,8	15,4	24,5	29,2	24,5	33,5	39,2	19,1	32,9	46,1	32,9	51,3	66,1	kbps
Tonal noise link budget	43,9	41,9	37,8	33,3	21,8	14,2	9,3	4,1	35,0	32,6	21,7	14,2	9,3	4,1	dB
Tonal in-band noise link budget	35,0	33,5	29,1	24,9	11,2	1,4	−3,2	−8,3	25,6	23,6	11,2	1,4	−3,2	−8,3	dB
Periodic impulse noise link budget	23,7	21,7	12,3	9,1	3,3	11,5	3,1	−2,9	12,3	8,7	3,3	11,1	3,1	−2,9	dB
Random impulse noise link budget	25,9	22,9	19,1	16,5	11,3	12,3	6,3	0,7	18,7	16,1	11,3	12,3	6,5	1,1	dB
Intentional communicator link budget	37,5	37,5	32,1	28,1	23,1	21,7	15,7	10,7	32,1	27,7	23,1	21,7	15,7	10,7	dB
Composite link budget (LB_{PHY})	42,2	40,8	36,3	33,4	27,9	27,9	22,9	18,5	35,6	33,0	27,9	27,9	22,9	18,6	dB
Composite in-band link budget	28,2	26,0	20,2	16,8	8,6	8,4	2,1	−3,5	18,9	16,1	8,6	8,3	2,1	−3,4	dB
der04 link budget	32,3	31,5	26,1	22,9	14,3	6,3	2,1	−3,3	25,9	22,9	14,1	6,3	2,1	−3,3	dB
der06 link budget	31,7	31,3	26,7	24,5	14,1	4,1	0,1	−4,7	26,9	24,5	14,1	4,1	0,3	−4,7	dB
der34 link budget	53,6	51,0	48,8	45,8	41,4	40,2	34,8	29,0	48,6	45,8	41,4	40,2	34,6	29,2	dB
der36 link budget	49,6	47,0	45,0	42,6	37,8	36,8	31,2	25,4	44,8	42,4	37,6	36,8	31,4	25,8	dB
der50 link budget	0,7	−1,9	−6,5	−8,9	−14,5	−16,7	−22,3	−27,7	−6,9	−9,5	−14,7	−16,7	−22,3	−27,7	dB
der51 link budget	6,0	3,6	−0,2	−2,8	−8,2	−10,0	−15,4	−20,8	−0,8	−3,2	−8,2	−10,2	−15,4	−20,8	dB
der average link budget	29,0	27,1	23,3	20,7	14,2	10,1	5,1	−0,4	23,1	20,5	14,1	10,1	5,1	−0,3	dB

* Header Type B is defined in PRIME 1.4 standard (not available for PRIME 1.3.6).

Table 5. Incremental results with the spline equalizer compared to the polynomial equalizer presented in [10] for PRIME 1.3.6 and 1.4.

	Header Type B *								Header Type A						
Parameter	Robust DBPSK	Robust DQPSK	DBPSK_CC	DQPSK_CC	D8PSK_CC	DBPSK	DQPSK	D8PSK	DBPSK_CC	DQPSK_CC	D8PSK_CC	DBPSK	DQPSK	D8PSK	Units
SNR required for AWGN	0,2	0,2	0,0	0,2	0,0	0,0	0,0	0,2	0,2	0,2	0,0	0,0	0,0	0,0	dB
Packet layer data rate (DRPKT)	0,0	0,0	0,0	0,0	0,0	0,0	0,0	0,0	0,0	0,0	0,0	0,0	0,0	0,0	%
Tonal noise link budget	5,4	8,9	5,8	6,0	4,1	0,0	0,0	0,0	4,3	5,2	4,1	0,0	0,0	0,0	dB
Tonal in-band noise link budget	6,0	10,8	7,3	8,5	5,1	0,0	0,0	0,0	5,4	7,1	5,2	0,0	0,0	0,0	dB
Periodic impulse noise link budget	−0,4	−0,2	0,0	0,0	0,2	0,0	0,0	0,0	0,0	−0,2	0,2	0,0	0,0	0,0	dB
Random impulse noise link budget	0,0	−0,2	−0,2	0,0	0,0	0,0	−0,2	−0,2	−0,4	−0,2	0,0	0,0	0,0	0,2	dB
Intentional communicator link budget	0,0	0,0	0,4	0,6	0,6	0,0	0,0	0,0	0,6	0,2	0,8	0,0	0,0	0,0	dB
Composite link budget (LBPHY)	1,0	1,7	1,2	1,3	1,0	0,0	0,0	0,0	0,9	1,0	1,0	0,0	0,0	0,0	dB
Composite in-band link budget	1,9	3,5	2,4	2,8	1,8	0,0	−0,1	−0,1	1,7	2,2	1,8	0,0	0,0	0,1	dB
der04 link budget	2,8	8,4	5,8	4,8	4,6	0,0	0,0	0,0	5,8	5,0	4,4	0,0	0,0	−0,2	dB
der06 link budget	4,4	9,0	8,0	7,8	6,4	0,0	0,0	0,2	8,2	7,8	6,2	0,0	0,2	0,2	dB
der34 link budget	0,0	0,2	0,0	−0,2	0,6	0,0	0,2	0,0	0,0	−0,2	0,6	0,0	0,0	0,0	dB
der36 link budget	0,2	0,0	0,0	0,0	0,6	0,0	0,0	−0,2	−0,2	0,0	0,4	0,0	0,2	0,0	dB
der50 link budget	−0,2	−0,2	−0,4	0,0	1,2	0,0	0,0	0,0	−0,6	−0,4	1,2	0,0	−0,2	0,0	dB
der51 link budget	0,0	−0,2	−0,2	−0,2	0,8	0,0	0,0	0,0	−0,6	−0,4	1,0	−0,2	−0,2	0,0	dB
der average link budget	1,2	2,9	2,2	2,0	2,4	0,0	0,0	0,0	2,1	2,0	2,3	0,0	0,0	0,0	dB

* Header Type B is defined in PRIME 1.4 standard (not available for PRIME 1.3.6).

As this proposal for PRIME equalization is an implementation option of the receiver, it does not affect the data rate of the transmitted signal. By contrast, the link budget experiences a 1.2 dB improvement.

As shown in Table 5, schemes without a convolutional encoder do not improve with the proposed new equalizer. The reason is that, despite the improvement of the equalizer, any disturbance affecting the pilot subcarriers introduces errors in the payload, and with no error correction, the reception of the frames fails.

With respect to the different types of disturbance, for the noise sources with the highest tonal component (ETSI tonal noises and der04, der06), modulations with a convolutional encoder show 6.6 dB improvement in their in-band metrics. This confirms the expectations about the Spline stability described in Section 3.1. By contrast, the average increase in their in-band metrics for these modulations is 0.1 dB in the case of non-tonal noises. Therefore, the subsequent analysis of the equalizer improvement is focused on modulation schemes with convolutional encoder and for the noises with high tonal components, where the performance enhancement is noticeable.

DBPSK and DQPSK PRIME 1.4 robust modes increment 7.3 dB their link budget for high tonal noises. Similarly, the equivalent non-robust modes with convolutional encoder show a 7.2 dB increase with respect to the implementation of a polynomial equalizer. Therefore, the equalizer performance is independent from the by-4 repetition mechanism. This is because the by-4 repetition is limited to the payload, so that pilot subcarriers used as data input for the equalizer remain untouched between robust and non-robust modes.

With the spline model, the link budgets of header type B modulations improve 6.9 dB for high tonal noises with convolutional encoder, while header type A modulations improve 6.1 dB. Header type A occupies two OFDM symbols, so it has 26 IQ points for the equalization, while header type B occupies four OFDM symbols, meaning 52 IQ points for the equalizer. The higher the number of the pilot subcarriers, the better the improvement of the spline-based equalizer, although it is non-proportional to the number of pilot subcarriers available.

Some situations, like the most robust modulations with ETSI periodic impulse, have a link budget decrease of 0.4 dB. This worsening is due to the higher degree of freedom of the spline. This also happens when AWGN is used as a reference, where the required SNR also increases slightly. This is the only drawback identified for this improvement proposal.

5.2. *PRIME: Reed–Solomon Encoding*

Table 6 summarizes the results introducing Reed–Solomon as an outer encoder, additional to the convolutional encoding mechanism. Table 7 represents the incremental results compared to Table 4, which gathers the performance results for PRIME including the improved spline curve model for the equalizer. This way, the absolute and incremental results offer a more accurate idea of the physical improvement under study.

Table 6. Absolute results with Reed–Solomon encoding for PRIME 1.3.6 and 1.4 (including the spline equalizer).

	Header Type B *								Header Type A						
Parameter	Robust DBPSK	Robust DQPSK	DBPSK_CC	DQPSK_CC	D8PSK_CC	DBPSK	DQPSK	D8PSK	DBPSK_CC	DQPSK_CC	D8PSK_CC	DBPSK	DQPSK	D8PSK	Units
SNR required for AWGN	−1,6	0,8	2,2	5,0	9,2	6,2	11,2	16,6	2,8	5,6	9,2	6,2	11,2	16,6	dB
Packet layer data rate (DRPKT)	4,2	7,7	14,0	22,1	27,4	23,3	30,6	39,2	17,6	30,7	41,9	30,7	51,3	66,1	kbps
Tonal noise link budget	44,5	42,8	39,5	34,9	25,6	18,9	15,9	14,9	35,6	33,7	25,6	19,3	16,1	15,1	dB
Tonal in-band noise link budget	35,2	34,3	30,6	26,3	15,9	7,5	5,5	5,3	25,8	24,6	15,9	8,3	5,7	5,7	dB
Periodic impulse noise link budget	24,1	22,3	12,9	9,5	4,7	12,1	4,3	−1,3	12,5	9,5	4,9	12,1	4,5	−1,3	dB
Random impulse noise link budget	26,3	23,9	20,9	17,7	13,7	16,3	10,9	5,7	19,9	17,3	13,5	16,1	10,9	5,9	dB
Intentional communicator link budget	37,5	37,5	33,5	31,5	26,1	26,3	20,5	15,3	33,5	30,3	25,7	26,3	20,1	15,3	dB
Composite link budget (LBPHY)	42,5	41,3	37,4	34,7	30,0	30,7	26,3	22,9	36,3	34,2	29,9	30,8	26,3	23,0	dB
Composite in-band link budget	28,5	26,8	21,5	17,8	11,4	12,0	6,9	3,2	19,4	17,1	11,4	12,2	7,0	3,4	dB
der04 link budget	33,5	31,7	27,5	25,1	17,7	15,5	10,5	9,3	27,5	24,9	17,9	15,9	11,1	9,3	dB
der06 link budget	33,5	33,3	29,3	26,1	17,7	13,1	8,1	7,1	29,3	25,9	17,7	13,1	8,3	7,1	dB
der34 link budget	54,8	51,6	50,2	46,8	42,8	46,2	40,6	35,2	49,8	46,6	42,8	46,2	41,0	35,6	dB
der36 link budget	51,0	48,2	46,4	43,2	39,0	42,6	37,0	31,6	45,8	43,4	39,4	42,6	37,0	31,8	dB
der50 link budget	1,5	−1,1	−4,5	−7,5	−12,1	−12,3	−16,5	−21,7	−5,1	−7,9	−12,3	−12,5	−16,5	−21,7	dB
der51 link budget	7,0	4,6	1,6	−1,4	−5,8	−5,6	−10,0	−15,0	0,8	−1,8	−6,0	−5,8	−9,8	−15,0	dB
der average link budget	30,2	28,1	25,1	22,1	16,6	16,6	11,6	7,8	24,7	21,9	16,6	16,6	11,9	7,9	dB

* Header Type B is defined in the PRIME 1.4 standard (not available for PRIME 1.3.6).

Table 7. Incremental results with Reed–Solomon encoding for PRIME 1.3.6 and 1.4 compared to Table 4.

	Header Type B *								Header Type A						
Parameter	Robust DBPSK	Robust DQPSK	DBPSK_CC	DQPSK_CC	D8PSK_CC	DBPSK	DQPSK	D8PSK	DBPSK_CC	DQPSK_CC	D8PSK_CC	DBPSK	DQPSK	D8PSK	Units
SNR required for AWGN	−0,6	−1,0	−1,0	−1,0	−1,8	−3,0	−3,4	−3,6	−0,8	−0,8	−1,8	−3,0	−3,4	−3,4	dB
Packet layer data rate (DR_{PKT})	−11,1	−13,4	−9,2	−9,7	−6,0	−5,1	−8,6	0,0	−7,7	−6,7	−9,2	−6,7	0,0	0,0	%
Tonal noise link budget	0,6	0,8	1,7	1,6	3,8	4,6	6,6	10,8	0,6	1,1	3,8	5,1	6,8	11,0	dB
Tonal in-band noise link budget	0,1	0,8	1,5	1,4	4,6	6,1	8,7	13,6	0,2	1,0	4,7	6,9	8,9	13,9	dB
Periodic impulse noise link budget	0,4	0,6	0,6	0,4	1,4	0,6	1,2	1,6	0,2	0,8	1,6	1,0	1,4	1,6	dB
Random impulse noise link budget	0,4	1,0	1,8	1,2	2,4	4,0	4,6	5,0	1,2	1,2	2,2	3,8	4,4	4,8	dB
Intentional communicator link budget	0,0	0,0	1,4	3,4	3,0	4,6	4,8	4,6	1,4	2,6	2,6	4,6	4,4	4,6	dB
Composite link budget (LB_{PHY})	0,3	0,5	1,1	1,3	2,1	2,8	3,4	4,4	0,7	1,1	2,0	2,9	3,4	4,4	dB
Composite in-band link budget	0,3	0,8	1,3	1,0	2,8	3,6	4,8	6,7	0,5	1,0	2,8	3,9	4,9	6,8	dB
der04 link budget	1,2	0,2	1,4	2,2	3,4	9,2	8,4	12,6	1,6	2,0	3,8	9,6	9,0	12,6	dB
der06 link budget	1,8	2,0	2,6	1,6	3,6	9,0	8,0	11,8	2,4	1,4	3,6	9,0	8,0	11,8	dB
der34 link budget	1,2	0,6	1,4	1,0	1,4	6,0	5,8	6,2	1,2	0,8	1,4	6,0	6,4	6,4	dB
der36 link budget	1,4	1,2	1,4	0,6	1,2	5,8	5,8	6,2	1,0	1,0	1,8	5,8	5,6	6,0	dB
der50 link budget	0,8	0,8	2,0	1,4	2,4	4,4	5,8	6,0	1,8	1,6	2,4	4,2	5,8	6,0	dB
der51 link budget	1,0	1,0	1,8	1,4	2,4	4,4	5,4	5,8	1,6	1,4	2,2	4,4	5,6	5,8	dB
der average link budget	1,2	1,0	1,8	1,4	2,4	6,5	6,5	8,1	1,6	1,4	2,5	6,5	6,7	8,1	dB

* Header Type B is defined in the PRIME 1.4 standard (not available for PRIME 1.3.6).

The PRIME link budget values including a Reed–Solomon outer encoder are 3.5 dB higher on average than the results without Reed–Solomon. It is an improvement for all the scenarios, with the drawback of decreasing the data transfer rate and increasing complexity in the transmitter and receiver.

Reed–Solomon implies a 6.1 dB average increase for modulation schemes without a convolutional encoder. In this scenario, introducing any coding mechanism has its maximum improvement. This is the key reason why this evolution to the PRIME standard would be interesting.

Opposed to the peak improvement of modulation schemes without a convolutional encoder, repetition by-4 robust modes have the lowest increase (0.8 dB). Having two encoding mechanisms already, convolutional encoding with repetition code has the consequence that adding Reed–Solomon as a third robustness mechanism has little margin for improvement.

Reed–Solomon impact is independent from the header type, both type A and type B headers have an average improvement of 3.9 dB. As Reed–Solomon coding is applied to the payload only, given that the header is robust enough to be decoded, the improvement introduced by Reed–Solomon is the same for both types of header.

If analyzed from the point of view of the different disturbance types, Reed–Solomon increases the link budget against every type of noise. Noise sources with the highest tonal component accumulate 5.3 dB improvement. Noises with high tonal component, combined with modulation schemes without convolutional encoder, accumulate 9.8 dB average improvement. Narrowband noises distort fewer subcarriers, but to a higher degree, which is directly related to the Reed–Solomon error recovery mechanism. Focusing on non-tonal noises, the link budget increase goes from 1 to 3.2 dB.

The convolutional encoder and Reed–Solomon can be compared as alternative coding and error correction mechanisms. Reed–Solomon has less overhead, so it offers higher values of packet layer data rate, whereas its link budget values are worse than the values using the convolutional encoder. In order to show this, modulations with similar data rates are compared. DQPSK_CC without Reed Solomon (Table 4) has 4.2 dB higher link budget than DBPSK with Reed Solomon (Table 6). In a similar way, D8PSK_CC without Reed–Solomon (Table 4) has 2 dB higher link budget than DQPSK with Reed–Solomon (Table 6). The most interesting scheme for this proposal is D8PSK with header Type A, with 5.7 dB link budget decrease in exchange for 43.4% increase in terms of data rate if compared to D8PSK_CC with header type A and without Reed–Solomon (see Table 4).

The packet layer data rate shows an average decrease of 6.7% when Reed–Solomon is introduced. This is a low price compared with the increase in the link budget observed. Reed–Solomon includes a fixed overhead of 16 bytes per frame. It should be noted that, in this study, a fixed payload of 256 bytes is used. In real applications, the data rate impact will statistically vary whether the overhead fits in the last symbol's padding or additional OFDM symbols are required.

5.3. G3-PLC: Tone Map

Table 8 presents the tone map results selected by the algorithm for each disturbance and physical configuration.

Table 8. Tone map selected per disturbance and physical configuration.

	Differential																							
	ROBO						**DBPSK**						**DQPSK**						**D8PSK**					
AWGN	1	1	1	1	1	1	1	1	1	1	1	1	1	1	1	1	1	1	1	1	1	1	1	1
Tonal noise 26 kHz	1	0	1	1	0	1	1	0	1	1	0	1	1	0	1	1	1	1	1	0	1	1	1	1
Tonal noise 31 kHz	1	1	0	0	1	1	0	1	0	0	1	1	1	1	0	1	1	1	1	1	0	1	1	1
Tonal noise 36 kHz	0	1	1	0	1	1	0	1	1	0	1	1	0	1	1	1	1	1	1	1	1	1	1	1
Tonal noise 41 kHz	0	1	1	1	0	0	0	1	1	1	0	1	1	1	1	1	1	1	0	1	1	1	1	1
Tonal noise 46 kHz	1	0	1	1	1	1	1	0	1	1	1	1	1	0	1	1	1	1	1	0	1	1	1	1
Tonal noise 51 kHz	1	0	1	1	1	1	1	0	1	1	1	1	1	0	1	1	1	1	1	0	1	1	1	1
Tonal noise 56 kHz	1	1	0	1	1	1	1	1	0	1	1	1	1	1	0	1	1	1	1	1	1	1	1	1
Tonal noise 61 kHz	0	1	0	1	1	1	1	1	0	1	1	1	1	1	0	1	1	1	1	1	1	1	1	1
Tonal noise 66 kHz	1	1	1	0	1	1	1	1	1	0	1	1	1	1	1	0	1	1	1	1	1	0	1	1
Tonal noise 71 kHz	1	1	1	0	1	1	1	1	1	0	1	1	1	1	1	0	1	1	1	1	1	0	1	1
Tonal noise 76 kHz	1	1	1	1	0	1	1	1	1	1	0	1	1	1	1	1	0	1	1	1	1	1	0	1
Tonal noise 81 kHz	1	1	1	1	0	1	1	1	1	1	0	1	1	1	1	1	0	1	1	1	1	1	0	1
Tonal noise 86 kHz	1	1	1	1	1	0	1	1	1	1	1	0	1	1	1	1	1	0	1	1	1	1	1	1
Tonal noise 91 kHz	1	1	1	1	1	0	1	1	1	1	1	0	1	1	1	1	1	0	1	1	1	1	1	1
Ruido tonal 96 kHz	1	1	1	1	1	1	1	1	1	1	1	0	1	1	1	1	1	0	1	1	1	1	1	0
Ruido tonal 101 kHz	1	1	1	1	1	1	1	1	1	1	1	1	1	1	1	1	1	1	1	1	1	1	1	0
Ruido tonal 106 kHz	1	1	1	1	1	0	1	1	1	1	1	1	0	1	1	1	0	0	1	1	1	1	1	1
Ruido tonal 111 kHz	1	1	1	1	1	1	1	1	1	1	1	0	1	1	1	1	1	0	1	1	1	1	1	0
Ruido tonal 116 kHz	1	1	1	1	1	1	0	0	1	0	1	0	0	0	1	1	1	0	1	1	1	1	1	0
Ruido tonal 121 kHz	1	1	1	1	1	1	1	1	1	1	1	1	1	1	1	1	0	1	1	1	1	1	0	1
Ruido tonal 126 kHz	1	1	1	1	1	1	0	0	1	1	0	1	0	1	1	1	0	1	1	1	1	1	0	1
Ruido tonal 131 kHz	1	1	1	1	1	1	0	1	1	0	1	1	0	1	1	1	1	1	0	1	1	0	1	1
Ruido tonal 136 kHz	0	1	1	0	1	1	0	0	1	0	1	0	1	1	1	1	1	1	1	1	1	1	1	1
Ruido tonal 141 kHz	0	0	0	1	1	1	0	1	0	1	1	1	0	1	1	1	1	1	0	1	1	1	1	1
Ruido tonal 146 kHz	0	0	0	1	1	1	0	0	1	1	1	1	1	0	1	1	1	1	1	0	1	1	1	1
Periodic impulsive noise	1	1	1	0	0	0	1	1	1	1	1	1	1	1	1	0	0	0	1	1	1	0	0	0
Random impulsive noise	0	0	0	0	1	1	0	0	0	0	1	1	0	0	0	0	1	1	0	0	0	0	1	1
Intercomunicador Estándar	0	1	1	0	1	1	0	1	1	0	1	1	0	1	1	0	1	1	0	1	1	0	1	1
Intercomunicador 160 kHz	0	0	0	0	1	1	0	0	0	0	1	1	0	0	0	0	1	1	0	0	0	0	1	1
Intercomunicador 240 kHz	1	1	1	1	1	1	1	1	0	0	0	0	1	1	0	0	1	1	1	1	1	1	1	1
Intercomunicador 400 kHz	1	1	0	1	1	1	1	1	1	1	1	1	0	0	0	1	0	0	0	0	0	1	1	0
Noise der04	1	1	1	1	1	0	0	1	0	1	1	0	0	1	1	1	1	0	0	1	1	1	1	0
Noise der06	1	1	1	1	1	0	0	1	0	1	1	0	0	1	1	1	1	0	0	1	1	1	1	0
Noise der34	0	1	0	1	1	1	0	1	1	1	1	1	0	1	1	1	1	1	0	1	1	1	1	1
Noise der36	0	1	0	1	1	1	0	1	0	1	1	1	0	1	1	1	1	1	0	1	1	1	1	1
Noise der50	0	0	0	0	1	1	0	0	0	0	0	1	0	0	0	0	0	1	0	0	0	0	1	1
Noise der51	0	0	0	0	1	1	0	0	0	0	0	1	0	0	0	0	0	1	0	0	0	0	0	1

	Coherent																							
	ROBO						**BPSK**						**QPSK**						**8PSK**					
AWGN	1	1	1	1	1	1	1	1	1	1	1	1	1	1	1	1	1	1	1	1	1	1	1	1
Tonal noise 26 kHz	1	0	0	1	0	1	1	0	1	1	0	1	1	0	0	1	0	1	1	0	1	1	0	1
Tonal noise 31 kHz	1	1	0	0	1	0	1	1	0	0	1	1	0	1	0	0	1	0	1	1	0	0	1	1
Tonal noise 36 kHz	0	1	1	0	1	1	0	1	1	0	1	1	0	1	1	0	0	1	0	1	1	1	1	1
Tonal noise 41 kHz	0	1	1	1	0	0	0	1	1	1	0	0	0	1	1	1	0	0	0	1	1	1	1	1
Tonal noise 46 kHz	0	0	1	1	1	1	0	0	1	1	1	1	0	0	1	1	1	1	1	0	1	1	1	1
Tonal noise 51 kHz	1	0	1	1	1	1	1	0	1	1	1	1	1	0	0	1	1	1	1	0	1	1	1	1
Tonal noise 56 kHz	1	1	0	1	1	1	1	1	0	1	1	1	1	0	0	1	1	1	1	1	0	1	1	1
Tonal noise 61 kHz	0	1	0	1	1	1	1	1	0	1	1	1	0	1	0	1	1	1	1	1	0	1	1	1
Tonal noise 66 kHz	1	1	1	0	1	1	1	1	1	0	1	1	1	1	0	0	1	1	1	1	1	0	1	1
Tonal noise 71 kHz	1	1	1	0	0	1	1	1	1	0	0	1	1	1	1	0	0	1	1	1	1	0	1	1
Tonal noise 76 kHz	1	1	1	1	0	1	1	1	1	1	0	1	1	1	1	1	0	1	1	1	1	1	0	1
Tonal noise 81 kHz	1	1	1	1	0	1	1	1	1	1	0	1	1	1	1	1	0	0	1	1	1	1	0	1
Tonal noise 86 kHz	1	1	1	1	1	0	1	1	1	1	1	0	1	1	1	1	1	0	1	1	1	1	1	0
Tonal noise 91 kHz	1	1	1	1	1	0	1	1	1	1	1	0	1	1	1	1	1	0	1	1	1	1	1	0
Ruido tonal 96 kHz	1	1	1	1	1	0	1	1	1	1	1	0	1	1	1	1	1	0	1	1	1	1	1	0
Ruido tonal 101 kHz	1	1	1	1	1	1	1	1	1	1	1	1	1	1	1	1	1	0	1	1	1	1	1	0
Ruido tonal 106 kHz	1	1	1	1	1	1	1	1	1	1	1	1	1	0	1	1	1	0	1	0	1	1	1	0
Ruido tonal 111 kHz	1	1	1	1	1	1	1	1	1	1	1	0	1	0	1	1	1	0	0	0	1	1	1	0
Ruido tonal 116 kHz	1	1	1	1	1	1	1	1	1	1	1	1	1	1	1	1	1	0	1	0	1	1	1	0
Ruido tonal 121 kHz	1	1	1	1	1	1	1	1	1	1	1	1	1	1	1	1	0	1	1	1	1	1	0	1
Ruido tonal 126 kHz	1	1	1	1	1	1	1	1	1	1	0	1	0	1	1	0	0	1	0	1	1	1	0	1
Ruido tonal 131 kHz	1	1	1	0	1	1	1	1	1	0	1	1	0	1	1	0	1	1	0	1	1	0	1	1
Ruido tonal 136 kHz	0	1	1	0	1	1	0	0	1	0	1	0	1	1	1	1	1	1	0	1	1	1	1	1
Ruido tonal 141 kHz	0	0	0	1	1	1	0	1	0	1	1	1	0	0	0	1	1	1	0	1	1	1	1	1
Ruido tonal 146 kHz	0	0	0	1	1	1	0	0	0	1	1	1	0	0	0	1	1	1	0	0	1	1	1	1
Periodic impulsive noise	1	1	0	0	0	0	1	1	1	1	1	1	1	1	1	1	1	1	1	1	1	1	1	1
Random impulsive noise	0	0	0	0	1	1	0	0	0	0	1	1	1	1	1	1	1	1	0	0	0	0	1	1
Intercomunicador Estándar	0	1	1	0	1	1	0	1	1	0	1	1	0	1	1	0	1	1	0	1	1	0	1	1
Intercomunicador 160 kHz	0	0	0	0	1	1	0	0	0	0	1	1	0	0	0	0	1	1	0	0	0	0	1	1
Intercomunicador 240 kHz	1	1	0	0	1	1	1	0	0	0	1	0	1	1	1	1	1	1	1	1	1	1	1	1
Intercomunicador 400 kHz	1	1	0	1	1	1	1	1	0	1	1	1	0	0	0	1	1	1	1	1	1	1	1	1
Noise der04	0	1	1	1	1	0	0	1	1	1	1	0	0	1	0	0	1	0	0	1	1	1	1	0
Noise der06	0	1	1	1	1	0	0	1	1	1	1	0	0	1	0	1	1	0	0	1	1	1	1	0
Noise der34	0	1	0	1	1	1	0	1	0	1	1	1	0	1	0	1	1	1	0	1	1	1	1	1
Noise der36	0	1	0	1	1	0	0	1	0	1	1	0	0	0	0	1	1	0	0	1	1	1	1	1
Noise der50	0	0	0	0	1	1	0	0	0	0	1	1	1	1	1	1	1	1	0	0	0	0	1	1
Noise der51	0	0	0	0	1	1	0	0	0	0	1	1	1	1	1	1	1	1	1	1	1	1	1	1

5.3.1. Standard Tone Map

Table 9 gathers the absolute results applying the tone map combinations in Table 8 to G3-PLC. Table 10 summarizes the incremental results compared to the G3-PLC performance results without the tone map implementation published in [10].

Table 9. Absolute results with the standard tone map implemented in G3-PLC.

		Differential				Coherent				
Parameter	Header	ROBO	DBPSK	DQPSK	D8PSK	ROBO	BPSK	QPSK	8PSK	Units
SNR required for AWGN	−3,6	−2,2	1,2	4,6	9,8	−3,6	−0,8	2,2	6,2	dB
Tonal noise link budget	46,7	46,1	43,3	30,4	21,3	46,0	44,6	42,8	31,9	dB
Tonal in-band noise link budget	39,7	39,4	36,2	22,7	10,8	39,2	37,6	36,0	22,7	dB
Periodic impulse noise link budget	29,3	28,6	26,1	26,1	18,1	27,6	27,6	27,1	19,1	dB
Random impulse noise link budget	26,9	26,8	25,3	21,8	17,3	26,8	26,3	19,3	20,3	dB
Intentional communicator link budget	41,5	41,5	38,5	39,0	38,5	41,5	39,0	39,0	38,5	dB
Composite link budget (LB_{PHY})	44,9	44,6	42,6	39,5	35,0	44,4	43,5	41,6	38,0	dB
Composite in-band link budget	32,0	31,6	29,2	23,5	15,4	31,2	30,5	27,5	20,7	dB
der04 link budget	30,3	29,5	28,5	26,5	23,5	29,0	28,0	27,0	25,0	dB
der06 link budget	30,7	29,3	28,8	27,8	24,8	28,8	28,3	27,8	25,8	dB
der34 link budget	57,2	56,4	52,4	48,4	43,4	56,4	55,4	51,9	46,4	dB
der36 link budget	52,8	52,0	48,5	44,5	39,5	52,5	51,0	46,0	42,5	dB
der50 link budget	2,1	1,7	0,2	−3,3	−8,3	1,7	1,2	−6,3	−5,8	dB
der51 link budget	7,8	7,4	5,4	1,9	−2,1	7,4	5,9	0,4	−4,1	dB
der average link budget	30,2	29,4	27,3	24,3	20,1	29,3	28,3	24,5	21,6	dB

Table 10. Incremental results with the standard tone map implemented in G3-PLC compared to the original implementation presented in [10].

	Differential				Coherent				
Parameter	ROBO	DBPSK	DQPSK	D8PSK	ROBO	BPSK	QPSK	8PSK	Units
SNR required for AWGN	0	0	0	0	0	0	0	0	dB
Tonal noise link budget	1,8	6,3	6,6	4,5	1,3	6,6	8,0	9,0	dB
Tonal in-band noise link budget	2,4	8,1	9,6	5,6	1,5	8,1	9,9	10,4	dB
Periodic impulse noise link budget	−0,5	0,0	4,6	2,2	−0,7	−0,1	0,2	−0,2	dB
Random impulse noise link budget	1,7	4,8	5,5	5,8	0,1	4,0	−0,4	5,4	dB
Intentional communicator link budget	0,0	0,0	8,5	12,0	2,2	0,5	3,5	8,6	dB
Composite link budget (LB_{PHY})	0,6	2,2	5,0	4,9	0,6	2,2	2,3	4,6	dB
Composite in-band link budget	1,2	4,3	6,6	4,5	0,3	4,0	3,2	5,2	dB
der04 link budget	0,6	1,2	5,6	6,8	0,1	0,7	1,3	5,7	dB
der06 link budget	0,0	0,9	5,1	9,3	0,3	1,2	1,5	5,5	dB
der34 link budget	0,6	2,6	6,4	6,4	−0,2	3,8	3,5	4,6	dB
der36 link budget	0,4	3,1	6,3	5,9	−0,1	3,8	2,0	4,9	dB
der50 link budget	2,0	4,9	6,0	6,6	0,0	4,3	−0,4	4,7	dB
der51 link budget	1,6	3,8	4,7	6,1	−0,2	2,7	−0,2	−0,1	dB
der average link budget	0,9	2,8	5,7	6,9	0,0	2,8	1,3	4,2	dB

Note that G3-PLC result tables include an additional column related to header robustness. G3-PLC improvement proposals under analysis are limited to payload data. Beyond the threshold established by the header robustness, the improvements in the payload will not be relevant. Header robustness is, therefore, an important specification for the analysis of these G3-PLC results.

The implementation of the standard tone map in G3-PLC introduces 3.4 dB of average improvement.

Link budget in presence of ETSI in-band noises increases 3.7 dB with the tone map whereas, under DER noises, it improves 3 dB. It is especially useful under narrowband tonal noises, as the tone map will not transmit data in those subcarriers affected by the noise. This way, for ETSI in-band tonal noises, it accumulates a 7 dB average increase of the link budget.

On the contrary, the most complex situations for the tone map are disturbances with a nearly flat spectrum pattern. A 0.5 dB decrease of the link budget is observed for ETSI periodic impulse noise, whose tone map is '000111'. This is because frames need to be longer to accommodate the payload and the probabilities of time impulse noises affecting the frame slightly increase.

Repetition by-4 robust modes with the tone map increase their link budget 0.6 dB, whereas non-robust modes improve 4.3 dB. It should be reminded that, by specification, the tone map is applied to non-robust modes only, i.e., the application to robust modes is for research purposes in this study. Robust modes present low improvement because the combination of the repetition mechanism with the interleaver provides high frequency diversity. Additionally, most of their errors are related to header decoding or payload alignment, where the tone map, which is applied to payload only, is not helpful.

The tone map improvement increases with the density of the modulation scheme. 8PSK differential and coherent modes have a 5.2 dB link budget increase, while BPSK modes improve 3.5 dB. The 8PSK modes have a higher SNR requirement because the distance between their constellation points is lower and, thus, lower amplitude noises have larger impact in these modulations. Consequently, the tone map technique becomes more efficient in these scenarios.

5.3.2. Reallocation of the Power Assigned to Inactive Tones

Table 11 represents the absolute results applying the tone map combinations (Table 8) to G3-PLC with the proposed power reallocation. Table 12 summarizes the incremental results compared to Table 9, i.e., G3-PLC performance results with a standard tone map implementation.

Table 11. Absolute results with a tone map power reallocation in G3-PLC.

		Differential				**Coherent**				
Parameter	Header	ROBO	DBPSK	DQPSK	D8PSK	ROBO	BPSK	QPSK	8PSK	Units
SNR required for AWGN	−3,6	−2,2	1,2	4,6	9,8	−3,6	−0,8	2,2	6,4	dB
Tonal noise link budget	46,7	46,1	44,6	30,6	21,3	46,0	44,8	44,3	32,1	dB
Tonal in-band noise link budget	39,7	39,5	37,7	23,0	11,0	39,2	37,8	37,5	23,0	dB
Periodic impulse noise link budget	29,3	28,9	26,1	26,1	20,9	28,1	27,5	27,1	19,1	dB
Random impulse noise link budget	26,9	26,9	26,7	25,3	22,3	26,9	26,9	19,7	23,9	dB
Intentional communicator link budget	41,5	41,5	38,7	39,1	38,5	41,5	39,3	39,3	38,5	dB
Composite link budget (LB_{PHY})	44,9	44,7	43,2	40,2	36,6	44,5	43,7	42,1	38,7	dB
Composite in-band link budget	32,0	31,8	30,2	24,8	18,1	31,4	30,7	28,1	22,0	dB
der04 link budget	30,3	29,5	28,7	27,5	25,3	28,9	28,3	27,3	26,1	dB
der06 link budget	30,7	29,7	29,1	28,7	26,3	29,1	28,5	27,9	26,3	dB
der34 link budget	57,2	56,4	53,4	49,4	44,6	57,0	56,4	53,6	47,4	dB
der36 link budget	52,8	52,6	50,2	45,6	40,6	52,6	52,2	50,2	43,4	dB
der50 link budget	2,1	2,1	1,7	1,5	−3,7	1,9	1,9	−5,9	−1,9	dB
der51 link budget	7,8	7,8	7,8	6,6	5,4	7,8	7,6	0,6	−4,0	dB
der average link budget	30,2	29,7	28,5	26,6	23,1	29,6	29,2	25,6	22,9	dB

On average, the proposed power usage reallocation for the G3-PLC tone map introduces 1.1 dB of improvement.

Comparing the column about the link budget of the header and the rest of Table 11, it can be noticed that, in many of the combinations of noise types and transmission configurations, the link budget of the header is no higher than the ones including the payload. This implies that, in those situations, the limiting factor is the decoding of the header, and no improvement on the payload, like the ones proposed about the tone map, will increase the final link budget. This is the case of the robust modes. Tone map power usage reallocation for repetition by-4 robust modes increases 0.2 dB their link budget. Comparing header and ROBO modes columns in Table 11 with the absolute results of this improvement, it is observed that header decoding limits are reached.

Table 12. Incremental results with a tone map power reallocation in G3-PLC compared to the standard tone map implementation (Table 9).

	Differential				Coherent				
Parameter	ROBO	DBPSK	DQPSK	D8PSK	ROBO	BPSK	QPSK	8PSK	Units
SNR required for AWGN	0	0	0	0	0	0	0	0,2	dB
Tonal noise link budget	0,0	1,3	0,1	0,0	0,0	0,2	1,5	0,2	dB
Tonal in-band noise link budget	0,1	1,4	0,3	0,2	0,0	0,2	1,5	0,3	dB
Periodic impulse noise link budget	0,3	0,0	0,0	2,8	0,5	−0,1	0,0	0,0	dB
Random impulse noise link budget	0,1	1,4	3,5	5,0	0,1	0,6	0,4	3,6	dB
Intentional communicator link budget	0,0	0,2	0,1	0,0	0,0	0,3	0,3	0,0	dB
Composite link budget (LB_{PHY})	0,1	0,6	0,7	1,6	0,1	0,2	0,4	0,8	dB
Composite in-band link budget	0,2	0,9	1,3	2,7	0,2	0,2	0,6	1,3	dB
der04 link budget	0,0	0,2	1,0	1,8	−0,1	0,3	0,3	1,1	dB
der06 link budget	0,4	0,3	0,9	1,5	0,3	0,2	0,1	0,5	dB
der34 link budget	0,0	1,0	1,0	1,2	0,6	1,0	1,7	1,0	dB
der36 link budget	0,6	1,7	1,1	1,1	0,1	1,2	4,2	0,9	dB
der50 link budget	0,4	1,5	4,8	4,6	0,2	0,7	0,4	3,9	dB
der51 link budget	0,4	2,4	4,7	7,5	0,4	1,7	0,2	0,1	dB
der average link budget	0,3	1,2	2,3	3,0	0,3	0,8	1,2	1,3	dB

Differential modes have 1.5 dB link budget increase while coherent modes improve 0.7 dB. These values are influenced by the tone map number of '0' selections per mode and the header decoding limits. It was expected a theoretical link budget increase according to Equation (1), with an increase of the power spectral density based on the number of '0'. Nevertheless, robust modulation schemes were close to the header decoding limits, so this power usage technique does not offer the expected improvement.

The performance of this tone map implementation shows a high dependency on the different noise types. The gain of redistributing the power of inactive tones will directly depend on the number of '0's of the tone map. ETSI periodic impulse noise and certain DER noises whose selected tone map is '000011' and '000001', where header decoding limits are not reached, have the highest link budget increase of 1.8 dB and 2.1 dB.

Another aspect to be considered is that regulated conducted emissions for electromagnetic compatibility tests to be performed to the transmitter device [28] will be more complex due to this tone map power usage reallocation. Results presented in this research process assume that all the power not used in subcarriers marked with '0' in the tone map can be reallocated in subcarriers marked with '1'. There are three emission limits to be considered:

- Specification limits: Narrowband PLC specifications require a minimum transmission level of 120 dBμV [12].
- Regulation limits: CENELEC regulation sets power transmission requirements for devices operating in the frequency range 3 kHz to 148.5 kHz [28].
- Technology limits: PLC amplifier and power supply design will have a limit for power transmission not to distort the signal or have thermal issues.

Focusing on CENELEC [28], it regulates in-band and out-of-band emission limits, which are tested in a laboratory setup with the help of a 50 Ω line impedance stabilization network (LISN). Figure 6 represents a hypothetical situation of a transmitter implementation whose signal spectrum for a tone map '111111' meets out-band quasi-peak emission limits [28], whereas tone map '011100' exceeds the regulation limit, and even more for tone map '010000'. This effect must be considered while designing and testing a hardware implementing this proposal, in order to be able to reallocate all the power and comply with out-of-band quasi-peak emission limits [28].

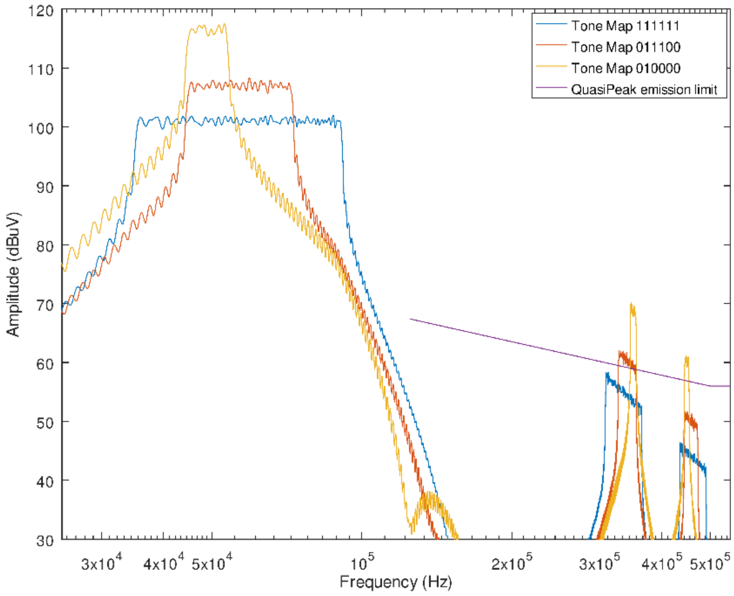

Figure 6. Possibility of not meeting emission levels permitted based on tone map values.

6. Conclusions

The simulation-based proposals analyzed in this paper for the physical layer of PRIME 1.3.6, PRIME 1.4, and G3-PLC technologies are proven to improve their response against disturbances present in the LV grid. PLC performance is enhanced with a combination of implementation improvements and modifications to the standards that could be included in future versions of PLC protocols.

Advanced metering infrastructure (AMI) deployments evolve to applications of higher complexity and innovation. PLC technologies that will enable these applications require robust testing and thorough performance analysis and evolution. The Virtual PLC Lab used in the present study has proven to be much more efficient than the conventional laboratory analog approach, saving a considerable amount of time and resources.

PRIME PLC technology performance and robustness increase when the improvements under analysis are introduced. A PRIME equalizer based on the spline curve model is more stable than the original polynomial curve model when adapting to channel responses impaired by tonal noises. Reed–Solomon makes PRIME modulation schemes without a convolutional encoder usable for real field scenarios. Reed–Solomon encoding is especially interesting for D8PSK without convolutional encoding.

The G3-PLC standard tone map increases the link budget for in-band tonal noises and its benefit is higher for high-density modulation schemes. The impact of the modification to the standard tone map using power reallocation in the link budget is related to the number of '0's in the tone map. The header robustness limit can be reached as the tone map is applied to the payload only, and CENELEC out-of-band emission levels [28] affected by the tone map with power reallocation must be considered for the hardware design of this option.

7. Future Work

As pointed out in [29], the smart grid is evolving in order to address the energy challenges of the society. The communication technologies will need to evolve in order to fulfill the requirements for this evolution. Therefore, more studies will be required to improve PLC technologies.

Further physical-level improvements can be studied oriented to communications robustness: using more complex coding schemes like low density parity check (LDPC) codes and turbo codes, or exploring adjustment options of OFDM parameters.

Improvements at higher levels can be studied. MAC layer mechanisms could be evolved improving the medium access algorithms or dynamic routing. Additionally, application layer bandwidth usage could be reduced, making the communication more robust.

Broadband powerline (BPL) communications technologies were originally designed for in-home communications. Adapting them in order to fulfill the smart grid requirements could provide increased throughput and reduced latency, in comparison with NB-PLC technologies. This could open the possibility for new applications beyond metering.

Author Contributions: Conceptualization: A.L., I.A., and D.d.l.V.; methodology, software, validation, formal analysis, and investigation: A.L.; resources, data curation: A.L. and I.A.; writing—original draft preparation: A.L.; writing—review and editing: I.A., L.M., D.d.l.V., and A.L.; visualization, supervision, project administration, and funding acquisition: A.L., I.A., and D.d.l.V. All authors have read and agreed to the published version of the manuscript.

Funding: This work was financially supported in part by the Basque Government under the grant numbers Elkartek KK-2018/00037 and IT1234-19, and by the Spanish Government under the grant RTI2018-099162-B-I00 (MCIU/AEI/FEDER, UE).

Conflicts of Interest: The authors declare no conflict of interest. The funders had no role in the design of the study; in the collection, analyses, or interpretation of data; in the writing of the manuscript; or in the decision to publish the results.

References

1. Prospex Research. *Europe's Top Twenty Power Industry Players 2016*; Prospex Research: Brighton, UK, 2016.
2. Dubey, A.; Mallik, R.K. PLC System Performance with AF Relaying. *IEEE Trans. Commun.* **2015**, *63*, 2337–2345. [CrossRef]
3. Sendin, A.; Berganza, I.; Arzuaga, A.; Pulkkinen, A.; Kim, I.H. Performance results from 100,000+ PRIME smart meters deployment in Spain. In Proceedings of the IEEE International Conference on Smart Grid Communications, Tainan, Taiwan, 5–8 November 2012; pp. 145–150. [CrossRef]
4. Sendin, A.; Llano, A.; Arzuaga, A.; Berganza, I. Field techniques to overcome aggressive noise situations in PLC networks. In Proceedings of the IEEE International Symposium on Power Line Communications and Its Applications, Udine, Italy, 3–6 April 2011; pp. 113–117. [CrossRef]
5. González-Sotres, L.; Mateo, C.; Frías, P.; Rodríguez-Morcillo, C.; Matanza, J. Replicability Analysis of PLC PRIME Networks for Smart Metering Applications. *IEEE Trans. Smart Grid* **2018**, *9*, 827–835. [CrossRef]
6. Matanza, J.; Alexandres, S.; Rodriguez-Morcillo, C. Performance evaluation of two narrowband PLC systems: PRIME and G3. *Comput. Stand. Interfaces* **2013**, *36*, 98–208. [CrossRef]
7. Arechalde, I.; Castro, M.; García-Borreguero, I.; Sendín, A.; Urrutia, I.; Fernandez, A. Performance of PLC communications in frequency bands from 150 kHz to 500 kHz. In Proceedings of the 2017 IEEE International Symposium on Power Line Communications and its Applications (ISPLC), Madrid, Spain, 3–5 April 2017; pp. 1–5. [CrossRef]
8. Kim, I.; Varadarajan, B.; Dabak, A. Performance Analysis and Enhancements of Narrowband OFDM Powerline Communication Systems. In Proceedings of the IEEE International Conference on Smart Grid Communications, Gaithersburg, MD, USA, 4–6 October 2010; pp. 362–367. [CrossRef]
9. Mölders, B.; Pletzer, T.M.; Wächter, M.; Koch, M. Experimental investigations of electrical influences on power line communication performance in distribution grid applications. In Proceedings of the CIRED Workshop 2016, Helsinki, Finland, 14–15 June 2016; pp. 1–4. [CrossRef]
10. Llano, A.; Angulo, I.; de la Vega, D.; Marron, L. Impact of channel disturbances on current narrowband Power Line Communications and lessons to be learnt for the future technologies. *IEEE Access* **2019**, *7*, 83797–83811. [CrossRef]
11. PRIME Alliance; Technical Working Group. *Specification for PoweRline Intelligent Metering Evolution v1.3.6*; PRIME Alliance: Brussels, Belgium, 2012.
12. PRIME Alliance. *Specification for PoweRline Intelligent Metering Evolution v1.4*; PRIME Alliance: Brussels, Belgium, 2014.
13. G3-PLC Alliance. *Narrowband OFDM PLC Specifications for G3-PLC Networks*; G3-PLC Alliance: Paris, France, 2015.

14. ITU-T. *G.9903: Narrowband Orthogonal Frequency Division Multiplexing Power Line Communication Transceivers for G3-PLC Networks*; Recommendation ITU-T G.9903; ITU-T: Geneva, Switcherland, 2017.
15. ETSI Technical Committee. *Power Line Telecommunications (PLT) Narrow Band Transceivers in the Range 9 kHz to 500 kHz Power Line Performance Test Method Guide ETSI Technical Committee Powerline Communications Technical Specification*; ETSI TS 103 909 V1.1.1 (2012-12); ETSI: Sophia Antipolis, France, 2012.
16. Şaylı, O.; Doğan, H.; Panayırcı, E. Spline interpolation based channel estimation for ACO-OFDM over visible light channels. In Proceedings of the 24th Signal Processing and Communication Application Conference (SIU), Zonguldak, Turkey, 16–19 May 2016; pp. 333–336. [CrossRef]
17. Llano, A.; Angulo, I.; Angueira, P.; Arzuaga, T.; de la Vega, D. Analysis of the Channel Influence to Power Line Communications Based on ITU-T G.9904 (PRIME). *Energies* **2016**, *9*, 39. [CrossRef]
18. Sendín, A.; Llano, A.; Angueira, P. Análisis de la utilización efectiva de los esquemas de modulación de las especificaciones PRIME para la lectura remota de contadores. In Proceedings of the XIX Telecom I+D, Madrid, Spain, 24–26 November 2009.
19. Reed, I.S.; Solomon, G. Polynomial Codes over Certain Finite Fields. *J. Soc. Ind. Appl. Math.* **1960**, 300–304. [CrossRef]
20. Hallak, G.; Niess, C.; Bumiller, G. Measurement Setup for Notch Evaluation of Narrowband PLC Devices. In Proceedings of the GLOBECOM 2017—2017 IEEE Global Communications Conference, Singapore, 4–8 December 2017; pp. 1–6. [CrossRef]
21. IEEE. *IEEE 1901.2-2013: IEEE Standard for Low-Frequency (Less than 500 kHz) Narrowband Power Line Communications for Smart Grid Applications*; IEEE: New York, NY, USA, 2013.
22. Llano, A.; Osorio, X.; de la Vega, D.; Angulo, I.; Arzuaga, T. Virtual Power-Line Communications Laboratory for technology development and research. In Proceedings of the REV2018 International Conference on Remote Engineering and Virtual Instrumentation, Dusseldorf, Germany, 16–19 May 2018; pp. 128–135.
23. Uribe-Pérez, N. Análisis de la Capacidad de PRIME para Gestión de Red en Entornos Con Generación Distribuida Y Sistemas de Almacenamiento. Ph.D. Thesis, Dept. Ingeniería de Comunicaciones, Universidad del País Vasco/Euskal Herriko Unibertsitatea, Bilbao, Spain, 2017.
24. Uribe-Pérez, N.; Angulo, I.; Hernández, L.; Arzuaga, T.; De La Vega, D.; Arrinda, A. Study of Unwanted Emissions in the CENELEC-A Band Generated by Distributed Energy Resources and Their Influence over Narrow Band Power Line Communications. *Energy J.* **2016**, *9*, 1007. [CrossRef]
25. ISO/IEC. *ISO/IEC 14908-3: Information Technology—Control Network Protocol—Part 3: Power Line*; ISO/IEC: Geneva, Switcherland, 2012.
26. The Centre for the Development of Renewable Energy Sources (CEDER) of the Research Centre for Energy, Environment and Technology (CIEMAT). Available online: http://www.ciemat.es/CEDERportal (accessed on 18 May 2019).
27. Fernandez, I.; Uribe-Pérez, N.; Eizmendi, I.; Angulo, I.; de la Vega, D.; Arrinda, A.; Arzuaga, T. Characterization of non-intentional emissions from distributed energy resources up to 500 kHz: A case study in Spain. *Int. J. Electr. Power Energy Syst.* **2019**, *105*, 549–563. [CrossRef]
28. CENELEC. *EN50065-1:2011. Specification for Signaling on Low-Voltage Electrical Installations in the Frequency Range 3 kHz to 148.5 kHz. General Requirements, Frequency Bands and Electromagnetic Disturbances*; ICS: 33.040.30.LB. CENELEC Standard: Brussels, Belgium, 2011. Available online: https://www.cenelec.eu/dyn/www/f?p=104:110:743346555655801::::FSP_ORG_ID,FSP_PROJECT,FSP_LANG_ID:821,22484,25 (accessed on 24 January 2020).
29. Zikria, Y.B.; Yu, H.; Afzal, M.K.; Rehmani, M.H.; Hahm, O. Internet of Things (IoT): Operating System, Applications and Protocols Design, and Validation Techniques. *Future Gener. Comput. Syst.* **2018**, *88*, 699–706. [CrossRef]